AIP | Applied Physics Letters

Interfacial electronic structure at the CH3NH3PbI3/MoOx interface

Peng Liu, Xiaoliang Liu, Lu Lyu, Haipeng Xie, Hong Zhang, Dongmei Niu, Han Huang, Cheng Bi, Zhengguo Xiao, Jinsong Huang, and Yongli Gao

Citation: Applied Physics Letters **106**, 193903 (2015); doi: 10.1063/1.4921339
View online: http://dx.doi.org/10.1063/1.4921339
View Table of Contents: http://scitation.aip.org/content/aip/journal/apl/106/19?ver=pdfcov
Published by the AIP Publishing

Interfacial electronic structure at the $CH_3NH_3PbI_3/MoO_x$ interface

Peng Liu,[1] Xiaoliang Liu,[1,a)] Lu Lyu,[1] Haipeng Xie,[1] Hong Zhang,[1] Dongmei Niu,[1] Han Huang,[1] Cheng Bi,[2] Zhengguo Xiao,[2] Jinsong Huang,[2] and Yongli Gao[3,a)]
[1]*Institute of Super-Microstructure and Ultrafast Process in Advanced Materials, College of Physics and Electronics, Central South University, Changsha 410083, People's Republic of China*
[2]*Department of Mechanical and Materials Engineering and Nebraska Center for Materials and Nanoscience, University of Nebraska-Lincoln, Lincoln, Nebraska 68588-0656, USA*
[3]*Department of Physics and Astronomy, University of Rochester, Rochester, New York 14627, USA*

(Received 25 March 2015; accepted 5 May 2015; published online 15 May 2015)

Interfacial electronic properties of the $CH_3NH_3PbI_3$ ($MAPbI_3$)/MoO_x interface are investigated using ultraviolet photoemission spectroscopy and X-ray photoemission spectroscopy. It is found that the pristine $MAPbI_3$ film coated onto the substrate of poly (3,4-ethylenedioxythiophene) poly(styrenesulfonate)/indium tin oxide by two-step method behaves as an n-type semiconductor, with a band gap of ~1.7 eV and a valence band edge of 1.40 eV below the Fermi energy (E_F). With the MoO_x deposition of 64 Å upon $MAPbI_3$, the energy levels of $MAPbI_3$ shift toward higher binding energy by 0.25 eV due to electron transfer from $MAPbI_3$ to MoO_x. Its conduction band edge is observed to almost pin to the E_F, indicating a significant enhancement of conductivity. Meanwhile, the energy levels of MoO_x shift toward lower binding energy by ~0.30 eV, and an interface dipole of 2.13 eV is observed at the interface of $MAPbI_3/MoO_x$. Most importantly, the chemical reaction taking place at this interface results in unfavorable interface energy level alignment for hole extraction. A potential barrier of ~1.36 eV observed for hole transport will impede the hole extraction from $MAPbI_3$ to MoO_x. On the other hand, a potential barrier of ~0.14 eV for electron extraction is too small to efficiently suppress electrons extracted from $MAPbI_3$ to MoO_x. Therefore, such an interface is not an ideal choice for hole extraction in organic photovoltaic devices. © *2015 AIP Publishing LLC*. [http://dx.doi.org/10.1063/1.4921339]

Recently, organometal halide perovskite materials such as methylammonium lead halides ($CH_3NH_3PbX_3$, X = I, Cl, Br) have arisen as one of the most attractive candidates for producing solar cells due to their high efficiency, cheap and abundant raw materials, and good scalability for industrial production.[1–8] Kojima *et al.*[9] first reported in 2009 on a 3.8% efficient solar cell with perovskite $CH_3NH_3PbI_3$ ($MAPbI_3$) and TiO_2. Grätzel *et al.*[10] brought the efficiency to 15% by depositing PbI_2 on nanoporous TiO_2 and subsequently submerging it into a CH_3NH_3I (MAI) solution. Using vapor deposition, Snaith's group[11] demonstrated that a planar heterojunction $MAPbI_3$ solar cell, without the mesoporous electrode in typical sensitized solar cells, could have very high efficiency of 15%. Yang's team[12] achieved an efficiency of 19.3% in $MAPbI_3$ solar cells by controlling the formation of the $MAPbI_3$ layer and careful choice of other materials. It is expected that the efficiency of 20% or higher can be reached by optimizing the device structures. The high performance of perovskite based solar cells had been partly ascribed to its very long carrier diffusion lengths by many authors. Snaith's group[13] reported a diffusion length exceeding 1 μm in a $MAPbI_3$ absorber. Huang's group[14] observed an electron-hole diffusion length of over 170 μm in solution-grown $MAPbI_3$ single crystals.

Many efforts have also been made to improve the charge transport and collection at the electrodes in organic devices. Transition metal oxide MoO_x has been extensively used as an insertion layer between the anode and the organic active materials in organic photovoltaic (OPV) cells[15–20] and organic light emitting diodes (OLED).[21–23] The high work function (WF) of MoO_x usually leads the highest occupied molecular orbital (HOMO) level of the contact organics bending-up toward the interface, which reduces the interface potential barrier and facilitates the hole extraction or injection at the interface. The encouraging performance enhancement has been demonstrated by many authors in small molecule OPV cells. Kröger *et al.*[24] proposed that the MoO_x interlayer at the anode tremendously enhanced hole injection into organic layer via electron extraction from the HOMO of organic layer through the MoO_x conduction band. Nakayama *et al.*[25] further inferred the origin of the hole injection enhancement by the MoO_x insertion layer. This line of work has recently been summarized by Wang *et al.*[26] Furthermore, MoO_x has also been demonstrated effective as an anode insertion layer in inorganic thin layer photovoltaic devices (IPV).[27] It is therefore highly desirable to investigate if MoO_x may serve the same role in perovskite based solar cells.

Here, we report our effort in investigating a $MAPbI_3/MoO_x$ interface, and addressing its electronic structure to verify whether or not such an interface is a potential candidate to enhance efficiently hole extraction in perovskite devices as in OPVs. Ultraviolet photoemission spectroscopy (UPS) and X-ray photoemission spectroscopy (XPS) data were collected as MoO_x was deposited layer by layer on $MAPbI_3$ film, and the interfacial chemistry and energy level alignment were measured to determine whether a deposited MoO_x insertion layer might serve as an injection/extraction layer between the anode and active layer as the case in OPVs. Our results

a)Electronic addresses: xl_liu@csu.edu.cn and ygao@pas.rochester.edu

indicate, however, the lack of chemical stability of the $MAPbI_3$ manifested by the strong interface reaction when MoO_x is deposited onto the $MAPbI_3$, as well as the energy levels mismatch between the MoO_x and the $MAPbI_3$, makes it not directly suitable for such insertion layers to be effective in $MAPbI_3$ based solar cells.

The $MAPbI_3$ film was fabricated by a two-step interdiffusion of spin-coated stacking layers of PbI_2 and MAI. Details about the $MAPbI_3$ film fabrication could be found elsewhere[28,29] We evaporated MoO_x layers on $MAPbI_3$ gradually and the thickness of the MoO_x film increased from submonolayer (0.5 Å) to several atom layers (64 Å) at a controlled rate of 0.2–0.3 Å/min were monitored by a quartz thickness monitor. At each MoO_x film thickness, we measured UPS and XPS spectra to learn the energy level alignment and interface reaction. The UPS was measured with He I (21.22 eV) and XPS with standard Al K_α X-ray source (1486.6 eV). A total energy resolution of 70 meV was selected for the UPS measurements as determined from the Fermi edge of Au. For XPS, the pass energy of the spectrometer with a resolution of 0.5 eV was 40 eV. The binding energies of all UPS and XPS spectra were calibrated and referenced to the Fermi level (E_F) of the analyzer. All measurements were taken at room temperature.

Shown in Figure 1 are the UPS spectra of evaporated MoO_x films on $MAPbI_3$ substrate. Figure 1(a) displays the evolution of secondary photoemission cut-off with the gradual deposition of MoO_x layers, from which we can know the WF of the sample surface. The WF was obtained from the energy difference between the secondary cut-off and the E_F of the system. For as-grown $MAPbI_3$, the WF was measured to be 4.13 eV, a little larger than other groups' reports.[30] It increased to 4.59 eV with the subsequent MoO_x deposition of 0.5 Å on $MAPbI_3$. Then it increased gradually, and finally saturated at 6.65 eV with the MoO_x deposition of 64 Å, resulting in a total WF increase of 2.52 eV. Interestingly, there was a sharp increase of WF between 4 Å and 12 Å, which could be possibly associated with a fully qualified MoO_x molecular layer formed at a certain thickness in this range. Figure 1(b) presents the UPS data of the highest lying valence band (VB) regions, in which the VB maximum (VBM) of $MAPbI_3$ film displays ~1.40 eV. A characteristic VB peak of MoO_x could be distinguished beyond a MoO_x coverage of 12 Å with the formation of a complete molecular layer of MoO_x. However, a shoulder peak was observed at ~4.43 eV with the MoO_x deposition of up to 1 Å, indicating a MoO_x VBM of 3.09 eV. With the subsequent deposition of up to 64 Å, the VBM shifted upward (to E_F) and finally saturated at about 2.78 eV, which indicated a total shift upward of ~0.3 eV.

To highlight the effect of the MoO_x thickness on the energy level shift, the detailed evolutions of the WF and VBM are shown in Figure 1(c) as the MoO_x thickness increases. It is clear that the WF and VBM change more rapidly until the MoO_x deposition of 16 Å; and then the changes become gradual at the following steps; finally, with the MoO_x deposition of over 32 Å, the shifts practically saturate. The shift of WF can be ascribed to the contributions of interface dipole and band-bending. The upward band-bending of the MoO_x VBM may be ascribed to less oxygen deficiencies in thicker MoO_x coverages than in thinner MoO_x ones, leading to a change from MoO^-_x to neutral MoO_x. It is consistent with our XPS data to be presented later, in which more Mo^{6+} was detected in thicker MoO_x coverages. Furthermore, it should be noted that at the first several steps, the ionization potential (IP) of MoO_x presents an upward tendency, which is associated with the chemical reaction in the interface region, in which the I component is reduced, possibly by passing the electron to MoO_x and becoming neutral. This can lead to the formation of volatile I that in turn escapes to the vacuum, resulting in the interface region no longer pure $MAPbI_3$.

In order to gain a better understanding of the energy levels evolution and the interface reaction, we used XPS to

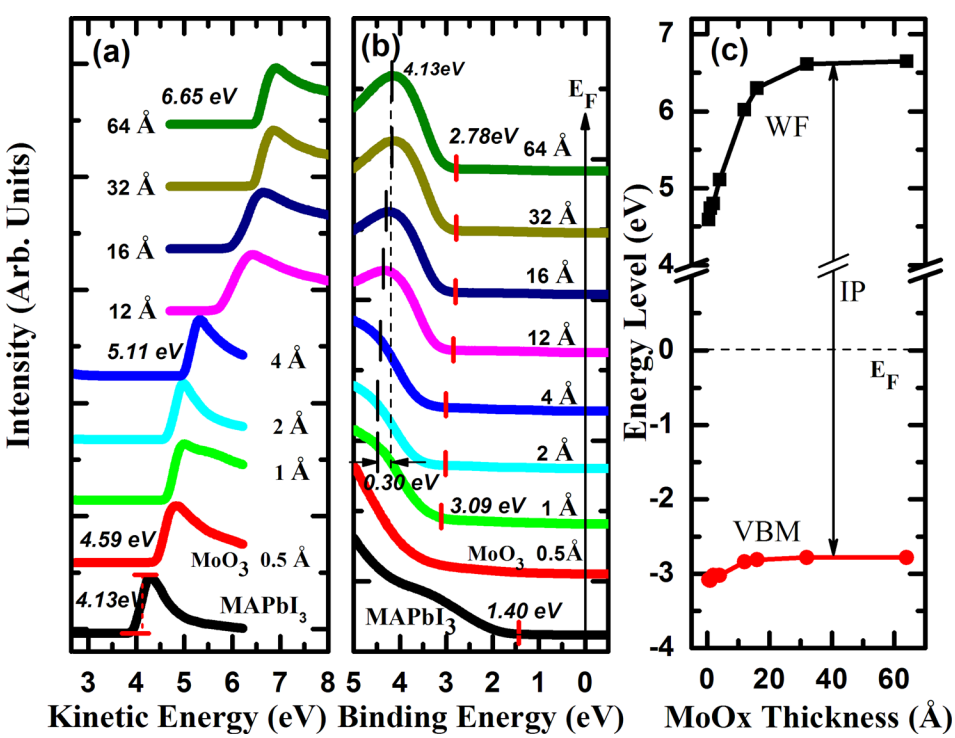

FIG. 1. Thickness dependent UPS data of MoO_x on $MAPbI_3$ film showing (a) the cut-off region and (b) the VBM region. (c) The evolution of WF and VBM as increasing the MoO_x thickness.

investigate further the chemical characteristics. Shown in Figure 2 are the XPS spectra of Pb $4f_{7/2}$, I $3d_{5/2}$, Mo 3d, and O 1s core levels in the $MAPbI_3/MoO_x$ interface as the MoO_x coverage increases. All the spectra were normalized to the same height for visual clarity. The information of the elements in $MAPbI_3$ substrate is just presented for low overlayer of MoO_x (up to 16 Å) due to the limit of XPS probing depth. From Figure 2(a), we can find that the Pb $4f_{7/2}$ core level comprises two components represented by two peaks which center on 138.59 eV and 136.80 eV, respectively. The bigger one (centered on 138.59 eV) can be associated to the Pb component in $MAPbI_3$, while the smaller one to the little metallic Pb decomposed from $MAPbI_3$, most likely due to the chemical reaction and sample annealing before the deposition of MoO_x film on it.[31] With the deposition of MoO_x on the $MAPbI_3$ substrate, both of the two peaks shift toward higher binding energies during the initial several steps of MoO_x deposition, accompanied with sharp intensity reduction. The total shift of Pb $4f_{7/2}$ is measured to be ~0.4 eV before it reaches saturation. Almost the same shift can be obtained for I 3d in Figure 2(b), which indicates a downward band bending of 0.4 eV in the energy levels of the $MAPbI_3$ film. However, the actual band bending should be rectified by incorporating the charging effect during the XPS measurement, which will be discussed further below. The C 1s spectrum of the pristine $MAPbI_3$ substrate (not showing here) mainly consists of two kinds of carbon components at 286.78 eV and 285.10 eV, respectively. The one at 286.78 eV (72%) can be attributed to the well-ordered and stoichiometric $MAPbI_3$, and the other (28%) from carbon impurities.

Shown in Figures 2(c) and 2(d) is the evolution of Mo 3d and O 1s XPS peaks, respectively. As a multivalence element, Mo has oxidation states 5+ and 6+ in our MoO_x film. The evaporated MoO_x films had been observed to be heavily n-type doped due to the oxygen deficiency[32] as we discussed previously. The difference of stoichiometric MoO_3 versus oxygen deficient MoO_x in devices has been reported by many authors.[19,33–35] Our experiment here also showed that the MoO_x films deposited on $MAPbI_3$ substrate in the vacuum was composed of Mo^{5+} and Mo^{6+}. We took the thickness of

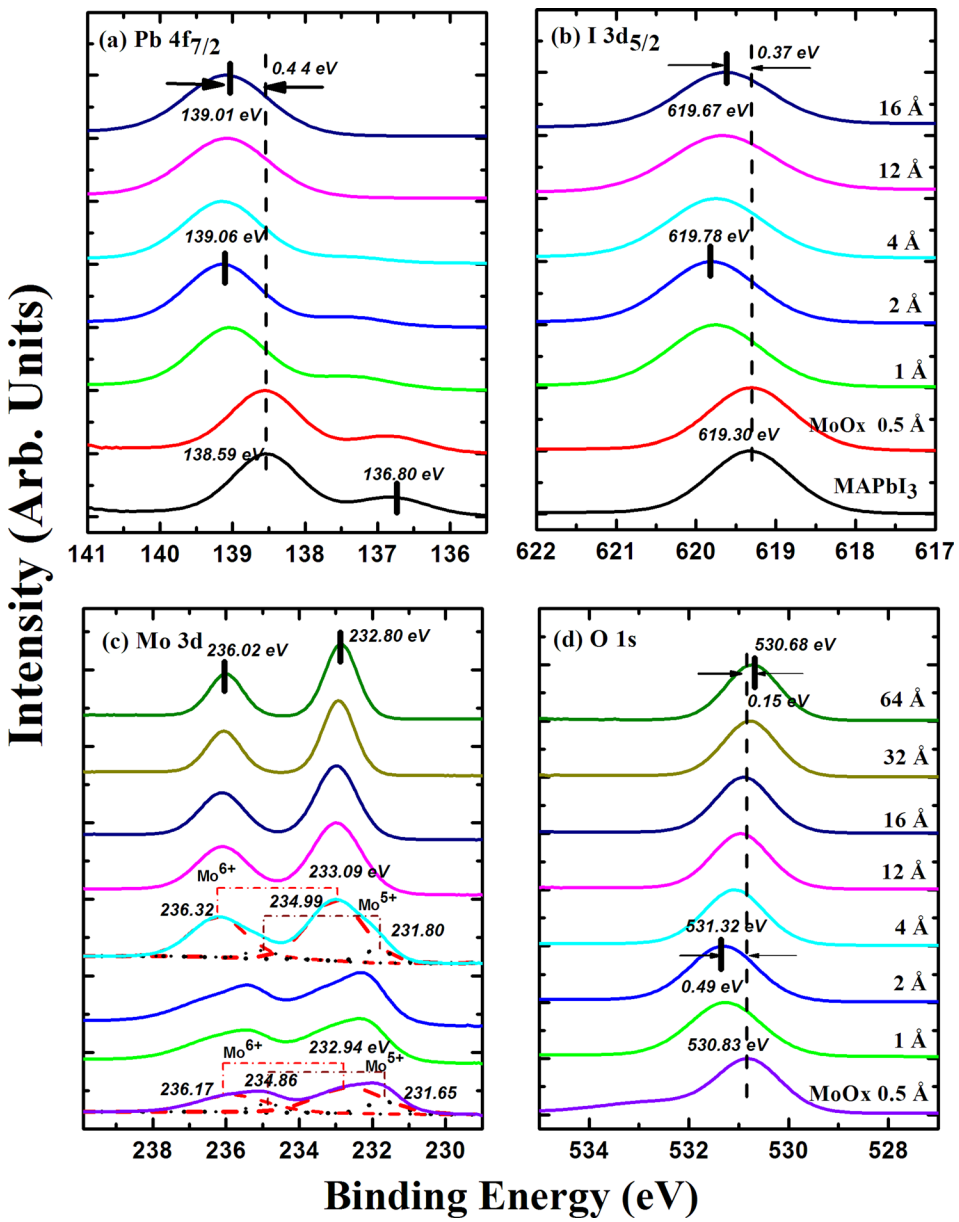

FIG. 2. XPS spectra of (a) Pb $4f_{7/2}$, (b) I $3d_{5/2}$, (c) Mo 3d, and (d) O 1s core levels of the $MAPbI_3/MoO_x$ interface as a function of increasing MoO_x layers. The dashed line and dotted line in (c) are the fitting of the experimental data using Mo^{6+} and Mo^{5+} Gaussian components.

MoO_x films at 0.5 Å and 4 Å to reveal the evolution of oxides species. For the MoO_x coverage of 0.5 Å, Mo 3d core level contains a pair of main peaks with a ~3.2 eV spin-orbit splitting between them, the one centered on ~235.1 eV belongs to Mo $3d_{3/2}$, and the other one centered on ~231.9 eV belongs to Mo $3d_{5/2}$. A pair of shoulder peaks appear at about 1.3 eV higher binding energy than their main peaks, which means a single doublet could not resolve the observed XPS spectra. From a fitting analysis with a Gaussian/Lorentzian mixing function, the positions of Mo $3d_{5/2}$ of two oxidation states of Mo, Mo^{6+}, and Mo^{5+}, are measured to be 232.94 eV (see dashed line) and 231.65 eV (see dotted line), respectively. The corresponding energy differences between the peak of Mo^{6+} and the peak of Mo^{5+} and the peak of O 1s are 297.89 eV and 299.18 eV, respectively. The results agree well with our previous reports,[26,36,37] in which the energy separations between the Mo $3d_{5/2}$ and O 1s are 297.8 eV and 299.1 eV for Mo^{6+} and Mo^{5+}, respectively.

We focus on the peak of Mo^{6+} with respect to Mo $3d_{5/2}$ in Figure 2(c), the peak position shifts from 232.94 eV with the deposition of 0.5 Å MoO_x to slightly higher binding energy at low MoO_x deposition of up to 2 Å, which could be ascribed to the charging effect during the XPS measurement, then it turns to shift toward lower BE with following deposition of MoO_x showing a saturation of 232.80 eV with 64 Å MoO_x coverage, indicating a total shift of ~0.15 eV toward the E_F. As shown in Figure 2(d), the position of the O 1s peak shows an approximately same shift as the Mo^{6+} peak of Mo $3d_{5/2}$. Therefore, a total band bending-up of ~0.15 eV in the MoO_x coverage is achieved with the MoO_x deposition of 64 Å. It is worth mentioning that this band bending-up is significantly smaller than the VBM shift upward of ~0.3 eV obtained by UPS in Figure 1(b). The difference of 0.15 eV between them can be most likely ascribed to the charging effect in XPS measurement, which is consistent with the result obtained by rectifying the core levels by reference to the C 1s of amorphous carbon. Therefore, the actual band bending-up of MoO_x film is ~0.30 eV after eliminating the charging effect. Similarly, in the underlying $MAPbI_3$ layer, the actual band bending-down should be ~0.25 eV after incorporating the charging effect into the shift of ~0.4 eV toward to higher band energy as shown in Figures 2(a) and 2(b).

The evolution of the ratio of Mo^{5+} to Mo^{6+} (Mo^{5+}/Mo^{6+}) is plotted in Figure 3(a) with increasing thickness of the MoO_x coverage. It is found that the fraction of Mo^{5+} is much less than that of Mo^{6+}. At the MoO_x deposition of 0.5 Å, the Mo^{5+}/Mo^{6+} ratio is about 0.24, then the fraction of Mo^{5+} begins to slightly increase accompanied with the decrease of Mo^{6+} with the following MoO_x deposition of up to 2 Å, leading to a slight increase of Mo^{5+}/Mo^{6+}. This may be due to electron transfer from perovskite to MoO_x. Such a transfer can lead I^- to neutral I, which subsequently leaves the surface because of the high vapor pressure as we discussed previously. Then, with the subsequent MoO_x deposition of up to 64 Å, the content of Mo^{5+} continuously decreases and only Mo^{6+} can be detected with the MoO_x deposition of beyond 12 Å. According to the change of intensity for Pb $4f_{7/2}$ and I $3d_{5/2}$, we observed that I signal drops much quicker than Pb. This is an evidence to confirm that I is leaving during the MoO_x deposition. Actually, as shown in Figure 3(b), the ratio of I to Pb (I/Pb) reduces from 2.15:1 of the pristine film to 0.67:1 after the deposition of 16 Å of MoO_x, indicating a significant deviation from the stoichiometry of $MAPbI_3$. Furthermore, the core levels of Mo 3d and O 1s shift to the opposite direction of I 3d and Pb 4f, a further evidence of perovskite decomposition in addition to the I:Pb ratio reduction. We obtained the ratios of Mo^{5+}/Mo^{6+} and I/Pb based on the XPS data by using Gaussian/Lorentzian fitting and incorporating atomic sensitivity factors.

The energy levels alignment diagram for the $MAPbI_3$/MoO_x interface is shown in Figure 3(c). The band gap of $MAPbI_3$ is taken as 1.7 eV according to our previous results[31,38] and the corresponding CBM of $MAPbI_3$ locates at ~0.30 eV above the E_F, which means the $MAPbI_3$ sample used here is heavily n-type material. The band gap of MoO_x is set as 3.2 eV by assuming the optical gap of MoO_x as the difference between its CB minimum and VBM. There is a band bending-down of 0.25 eV in the underlying $MAPbI_3$ layer, while a band bending-up of ~0.64 eV for the vacuum level and a band bending-up of ~0.30 eV for the VBM in the MoO_x overlayer with enough thickness of the MoO_x deposition. An interface dipole of ~2.13 eV observed at $MAPbI_3$/MoO_x interface can be attributed to the electron transfer from the lower WF material $MAPbI_3$ to the higher WF material MoO_x.

Given that $MAPbI_3$ is used as absorber layer to provide charge carriers in OPV devices, while MoO_x is used as anode buffer layer to efficiently enhance hole transport and suppress electron transport. Therefore, it is interesting to discuss the potential barrier of the $MAPbI_3/MoO_x$ interface for hole and electron transfer. It is observed that there is a potential barrier of 1.36 eV for hole extraction from $MAPbI_3$ to MoO_x due to the offset between their VBMs, which will impede the hole extraction rather than enhance it. On the other hand, a small potential barrier of ~0.14 eV for electron extraction is achieved due to the offset between their CBMs, which is too low to suppress the electron extraction from $MAPbI_3$ to MoO_x. Therefore, we can conclude that such an interface does not provide a favorable energy level alignment to exclusively collect holes. Actually, the $MAPbI_3/MoO_x$ interface is not an ideal choice for hole extraction in OPV devices. Some special hole transfer materials should be inserted between the $MAPbI_3$ layer and the MoO_x layer not only to achieve the favorable energy level alignment, thus to fulfill the Ohm contact, but also to suppress the chemical reaction between them.

In conclusion, we have investigated the interfacial electronic properties of the interface of $MAPbI_3/MoO_x$ using UPS and XPS. The energy levels of $MAPbI_3$ shifted toward higher binding energy by 0.25 eV with the MoO_x overlayer of 64 Å upon it, which can be ascribed to the electron transfer from $MAPbI_3$ to MoO_x. Meanwhile, the energy levels of the MoO_x coverage shifted upward by 0.30 eV, and an interface dipole of ~2.13 eV was observed at the $MAPbI_3/MoO_x$ interface. Most importantly, the chemical reaction taking place at such an interface, exemplified by the rapid reduction of iodine after MoO_x deposition, results in unfavorable interface energy level alignment for hole extraction. The potential barrier of 1.36 eV for hole extraction was too big to efficiently transfer holes from $MAPbI_3$ to MoO_x, while the

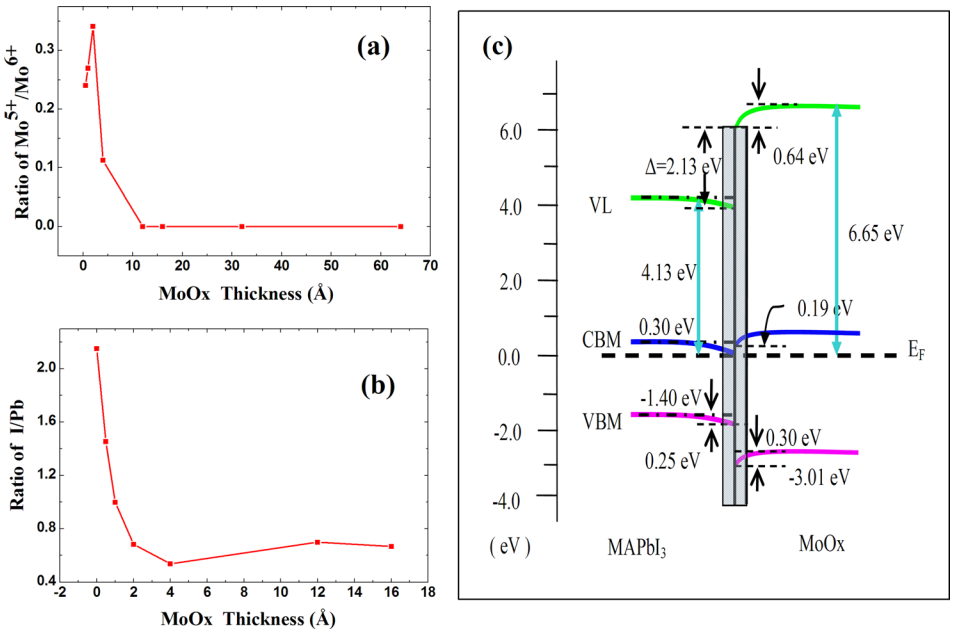

FIG. 3. The ratio of (a) Mo^{5+}/Mo^{6+} and (b) I/Pb with increasing thickness of the MoO_x coverage. (c) The energy levels alignment diagram at the $MAPbI_3/MoO_x$ interface.

potential barrier of ~0.14 eV for electron extraction was too small to efficiently suppress electrons extracted from $MAPbI_3$ to MoO_x. Therefore, it is concluded that the $MAPbI_3/MoO_x$ interface is not an ideal choice for hole extraction in OPV devices.

We thank the financial support by the National Science Foundation (Grant No. CBET-1437656) and the National Natural Science Foundation of China (Grant Nos. 51173205 and 11334014). J. Huang thanks the financial support by the National Science Foundation under Award Nos. ECCS-1252623 and ECCS-1201384, and Defense Threat Reduction Agency under Award No. HDTRA1-14-1-0030.

[1]M. A. Green, A. Ho-Baillie, and H. J. Snaith, Nat. Photonics **8**, 506 (2014).
[2]N. J. Jeon, J. H. Noh, Y. C. Kim, W. S. Yang, S. Ryu, and S. Seok, Nat. Mater. **13**, 897 (2014).
[3]N. J. Jeon, J. H. Noh, W. S. Yang, Y. C. Kim, S. Ryu, J. Seo, and S. Seok, Nature **517**, 476 (2015).
[4]J.-H. Im, I.-H. Jang, N. Pellet, M. Grätzel, and N.-G. Park, Nat. Nanotechnol. **9**, 927 (2014).
[5]Z. G. Xiao, Y. B. Yuan, Y. C. Shao, Q. Wang, Q. F. Dong, C. Bi, P. Sharma, A. Gruverman, and J. S. Huang, Nat. Mater. **14**, 193 (2015).
[6]J. Burschka, N. Pellet, S.-J. Moon, R. Humphry-Baker, P. Gao, M. K. Nazeeruddin, and M. Grätzel, Nature **499**, 316 (2013).
[7]M. Liu, M. B. Johnston, and H. J. Snaith, Nature **501**, 395 (2013).
[8]D. Liu and T. L. Kelly, Nat. Photonics **8**, 133 (2014).
[9]A. Kojima, K. Teshima, Y. Shirai, and T. Miyasaka, J. Am. Chem. Soc. **131**, 6050 (2009).
[10]U. Bach, D. Lupo, P. Comte, J. E. Moser, F. Weissortel, J. Salbeck, H. Spreitzer, and M. Grätzel, Nature **395**, 583 (1998).
[11]J. M. Ball, M. M. Lee, A. Hey, and H. J. Snaith, Energy Environ. Sci. **6**, 1739 (2013).
[12]H. Zhou, Q. Chen, G. Li, S. Luo, T.-B. Song, H.-S. Duan, Z. Hong, J. You, Y. Liu, and Y. Yang, Science **345**, 542 (2014).
[13]S. D. Stranks, G. E. Eperon, G. Grancini, C. Menelaou, M. J. P. Alcocer, T. Leijtens, L. M. Herz, A. Petrozza, and H. J. Snaith, Science **342**, 341 (2013).
[14]Q. Dong, Y. Fang, Y. Shao, P. Mulligan, J. Qiu, L. Cao, and J. Huang, Science **347**, 967 (2015).
[15]J. Meyer, K. Zilderberg, T. Riedl, and A. Kahn, J. Appl. Phys. **110**, 033710 (2011).
[16]V. Shrotriya, G. Li, Y. Yao, C. W. Chu, and Y. Yang, Appl. Phys. Lett. **88**, 073508 (2006).
[17]H. Wang, Z. Liu, M. F. Lo, T. W. Ng, C.-S. Lee, D. Yan, and S.-T. Lee, J. Appl. Phys. **107**, 024510 (2010).
[18]Irfan, M. Zhang, H. Ding, C. W. Tang, and Y. Gao, Org. Electron. **12**, 1588 (2011).
[19]X. L. Liu, C. G. Wang, I. Irfan, S. J. Yi, and Y. Gao, Org. Electron. **15**, 977 (2014).
[20]X. Liu, S. Yi, C. Wang, C. Wang, and Y. Gao, J. Appl. Phys. **115**, 163708 (2014).
[21]S. Tokito, K. Noda, and Y. Taga, J. Phys. D: Appl. Phys. **29**, 2750 (1996).
[22]X. L. Liu, C. G. Wang, C. C. Wang, I. Irfan, and Y. Gao, Org. Electron. **17**, 325 (2015).
[23]J. Hou, J. Wu, Z. Xie, and L. Wang, Appl. Phys. Lett. **95**, 203508 (2009).
[24]M. Kröger, S. Hamwi, J. Meyer, T. Riedl, W. Kowalsky, and A. Kahn, Appl. Phys. Lett. **95**, 123301 (2009).
[25]Y. Nakayama, K. Morii, Y. Suzuki, H. Machida, S. Kera, N. Ueno, H. Kitagawa, Y. Noguchi, and H. Ishii, Adv. Funct. Mater. **19**, 3746 (2009).
[26]C. Wang, I. Irfan, X. Liu, and Y. Gao, J. Vac. Sci. Technol., B **32**, 040801 (2014).
[27]M. Zhang, Irfan, H. Ding, Y. Gao, and C. W. Tang, Appl. Phys. Lett. **96**, 183301 (2010).
[28]Q. Wang, Y. Shao, H. P. Xie, L. Lyu, X. Liu, Y. Gao, and J. Huang, Appl. Phys. Lett. **105**, 163508 (2014).
[29]Z. Xiao, C. Bi, Y. Shao, Q. Dong, Q. Wang, Y. Yuan, C. Wang, Y. Gao, and J. Huang, Energy Environ. Sci. **7**, 2619 (2014).
[30]P. Schulz, E. Edri, S. Kirmayer, G. Hodes, D. Cahen, and A. Kahn, Energy Environ. Sci. **7**, 1377 (2014).
[31]R. Lindblad, D. Bi, B. Park, J. Oscarsson, M. Gorgoi, H. Siegbahn, M. Odelius, E. M. J. Johansson, and H. Rensmo, J. Phys. Chem. Lett. **5**, 648 (2014).
[32]M. Kröger, S. Hamwi, J. Meyer, T. Riedl, W. Kowalsky, and A. Kahn, Org. Electron. **10**, 932 (2009).
[33]M. P. Ramuz, M. Vosgueritchian, P. Wei, C. Wang, Y. Gao, Y. Wu, Y. Chen, and Z. Bao, ACS Nano **6**, 10384 (2012).
[34]M. Vasilopoulou, L. C. Palilis, D. G. Georgiadou, P. Argitis, S. Kennou, L. Sygellou, I. Kostis, G. Papadimitropoulos, N. Konofaos, A. A. Iliadis, and D. Davazoglou, Appl. Phys. Lett. **98**, 123301 (2011).
[35]M. T. Greiner, M. G. Helander, Z. B. Wang, W. M. Tang, J. Qiu, and Z. H. Lu, Appl. Phys. Lett. **96**, 213302 (2010).
[36]C. Wang, A. J. Turinske, and Y. Gao, Appl. Phys. B **113**, 361 (2013).
[37]I. Irfan and Y. Gao, J. Photonics Energy **2**, 021213 (2012).
[38]X. L. Liu, C. G. Wang, L. Lyu, C. C. Wang, Z. G. Xiao, C. Bi, J. S. Huang, and Y. Gao, Phys. Chem. Chem. Phys. **17**, 896–902 (2015).